From C_{60} to a fullerene tube: Systematic analysis of lattice and electronic structures by the extended Su-Schrieffer-Heeger model

Kikuo Harigaya*
Fundamental Physics Section, Physical Science Division, Electrotechnical Laboratory, Umezono 1-1-4, Tsukuba, Ibaraki 305, Japan
(Received 25 November 1991)

The development from C_{60} and C_{70} to an infinitely long tube is studied by changing the carbon number N. The extended Su-Schrieffer-Heeger Hamiltonian is applied to various geometrical structures and solved for the half-filling case of π electrons. For finite N (~ 100), appreciable dimerizations (~ 0.01 Å) exist, and a fairly large gap (~ 0.1–1 eV) remains. The solution, which includes the perfect Kekulé structure, always gives the lowest energy. Other solutions, where there are deviations from the Kekulé structure, have higher energies. When N goes to infinity, the strength of the unique dimerization pattern, i.e., the prefect Kekulé structure, becomes too small to be observed, but the gap width ($\simeq 0.02$ eV) is comparable to room temperature and can be measured. Therefore, the infinitely long tube will have properties like those of semiconductors with a very narrow gap. We would not expect perfect metallic properties, but peculiar properties due to the small gap could be observed in experiments.

I. INTRODUCTION

The fullerenes C_N, which are a new category of mesoscopic carbon molecules, have been investigated intensively. C_{60} has a spherical shape while C_{70} has an ellipsoid shape. Quite recently, another category of mesoscopic carbon molecules, "fullerene tubes," has been synthesized by the arc-discharge evaporation method, and the structure has been revealed by an electron microscope.[1] They have cylindrical shapes. The surface of the cylinder has a honeycomb-lattice pattern just as in a two-dimensional graphite plane.

In a series of publications,[2–4] we have extended the Su-Schrieffer-Heeger (SSH) model[5] of polyacetylene to C_{60} and C_{70}. We have analyzed the lattice and electronic structures by a numerical iteration method, taking into account the full lattice relaxation. For the undoped case, the well-known bond-alternation patterns and energy-level structures[6,7] have been found to be reproduced even by the simple electron-phonon model. In C_{60},[2,6] the highest occupied molecular orbital (HOMO) is fivefold degenerate, while the lowest unoccupied molecular orbital (LUMO) is threefold degenerate. This is due to the high icosahedral symmetry. There are ten short bonds and twenty long bonds in C_{60}. In C_{70},[3,7] the HOMO and LUMO are nondegenerate, owing to the structural perturbation from C_{60} to C_{70}. In the electron- and hole-doped systems (C_{60} and C_{70}),[2–4] two nondegenerate levels intrude largely into the energy gap. Furthermore, the lattice distorts and the dimerization becomes weaker along the equatorial line of the molecule. These are the "polaron" excitation in the fullerenes. The results of the polarons agree with the same calculations of the electron-doped C_{60} by Friedman.[8] The calculated optical absorption coefficient has predicted a peak at a lower energy than the energy gap.

The electronic properties of fullerene tubes, which have been recently discovered, are not well known. A recent theoretical work[9] has proposed properties between those of graphite and polyacetylene: there would be a bond alternation pattern but the dimerization would be much smaller than those in polyacetylene and C_{60}. It is also expected that the energy gap would be much smaller than in those systems. Other works[10] have shown that the gap can be wide (~ 1 eV), much smaller, or negligible, depending upon the structures of the tubes, i.e., the diameter and pitch of the helix.

The purpose of the present paper is to investigate the lattice and electronic properties of fullerene tubes, bearing in mind their relation to fullerenes with finite numbers of carbon atoms. Particularly, variations of dimerization and electronic properties, from C_{60} and C_{70} to an infinite tube, are analyzed systematically. The idea of a systematic investigation is as follows. We start from C_{60}. We cut C_{60} into two parts along an equatorial line of the sphere. After inserting ten carbon atoms and making bonds, we obtain the lattice geometry of C_{70}. We shall generalize the process of making C_{70} from C_{60}, in order to finally obtain a fullerene tube. If thirty carbons are inserted after cutting C_{60}, and each ten of them are arranged in a ring, we get a possible structure of C_{90}. The structure is depicted in Fig. 1(b). If ten more carbons are included, we obtain C_{100}, shown in Fig. 1(c). Furthermore, if ten more or twenty more carbons are added to the C_{100}, we get a C_{110} or C_{120}, depicted in Figs. 1(d) and 1(e). The molecule becomes longer and longer. Iterating these processes, we will finally obtain an infinitely long tube, where ten carbons are arranged in a ring perpendicular to the axis. The structure is shown in Fig. 1(a). Note that the alternation of short and long bonds depicted in Fig. 1 will be discussed in Sec. III. In experiments, helical structures are observed,[1] and there are various possible pitches for the helix. But, we consider only a nonhelical structure, because we are at the first stage of the investigation of the dispersion relations for the tubes and can expect interesting properties due to the Peierls

instability for the simple structure of a one-dimensional unit cell. Effects of the helical structures are left for future investigations.

This paper is organized as follows. We explain the model and numerical procedures in Sec. II. The development of lattice and electronic structures from C_{60} to a tube is investigated in Sec. III. Finite systems are numerically studied and results are extrapolated to an infinitely long tube. Section IV is devoted to tubes with a periodic boundary condition. Extrapolations to the infinite carbon number are performed and compared with the results of Sec. III. We close the paper with several remarks in Sec. V.

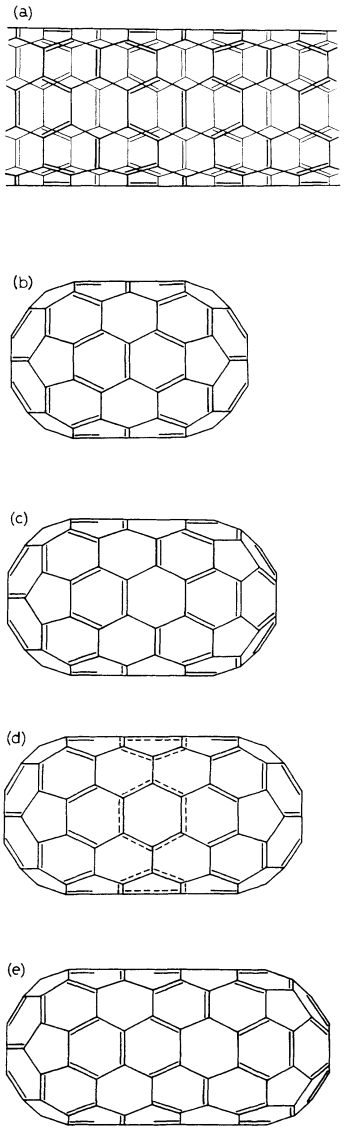

FIG. 1. Lattice configurations of (a) an infinitely long tube and (b)–(e) tubes with finite carbon numbers. In (a), front and back views are shown using normal and thin lines, respectively. In (b)–(e), only front views are shown for simplicity. The double and single lines indicate short and long bonds, respectively. In (d), several bonds cannot be classified into short and long bonds. They are shown by dashed lines.

II. MODEL

In previous papers,[2–4] the SSH model was extended to C_{60} and C_{70} molecules. In the present study, we apply the same model to fullerene tubes, making use of possible lattice geometries. The form of the model is

$$\mathcal{H}=\sum_{\langle ij\rangle,s}[-t_0+\alpha(u_i^{(j)}+u_j^{(i)})](c_{i,s}^{\dagger}c_{j,s}+\text{H.c.})+\frac{K}{2}\sum_{\langle ij\rangle}(u_i^{(j)}+u_j^{(i)})^2 . \tag{2.1}$$

In the first term, the quantity t_0 is the hopping integral of the ideal undimerized systems; α is the electron-phonon coupling; the operator $c_{i,s}$ annihilates a π electron at the ith carbon atom with spin s; $u_i^{(j)}$ is the displacement of the ith atom in the direction opposite to the jth atom (three $u_i^{(j)}$ for the given i are independent with each other); the sum is taken over nearest-neighbor pairs $\langle ij\rangle$. The quantity $u_i^{(j)}+u_j^{(i)}$ is the change of length of the bond between the ith and jth atoms. When it is positive, the bond length becomes longer and the hopping integral decreases from t_0; accordingly we take the sign before α to be negative. The second term is the elastic energy of the phonon system; the quantity K is the spring constant.

The model Eq. (2.1) is solved by the adiabatic approximation for phonons. The Schrödinger equation for π electron is

$$\varepsilon_\kappa\phi_{\kappa,s}(i)=\sum_{\langle ij\rangle}(-t_0+\alpha y_{i,j})\phi_{\kappa,s}(j) , \tag{2.2}$$

where ε_κ is the eigenvalue of the κth eigenstate and $y_{i,j}=u_i^{(j)}+u_j^{(i)}$ is the bond variable. The self-consistency equation for the lattice is

$$y_{i,j}=-\frac{2\alpha}{K}\sum_{\kappa,s}{}'\phi_{\kappa,s}(i)\phi_{\kappa,s}(j)+\frac{2\alpha}{K}\frac{1}{N_b}\sum_{\langle kl\rangle}\sum_{\kappa,s}{}'\phi_{\kappa,s}(k)\phi_{\kappa,s}(l) , \tag{2.3}$$

where the prime means the sum over the occupied states, the last term is due to the constraint $\sum_{\langle ij\rangle}y_{i,j}=0$, and N_b is the number of π bonds. It is 1.5 times the number of sites N, because three bonds are connected to each carbon atom. In polyacetylene,[11] $N_b=N$ has been used due to two bonds from each carbon. The constraint has been necessary in order to numerically obtain a correct dimerized ground state for the undoped system. We can confidently assume that the constraint works well for the present systems, too. Owing to the constraint, we can avoid the contraction of the lattice; the total bandwidth does not vary from that of the undimerized system.

A numerical solution is obtained in the following way.

(i) Random numbers between $-y_0$ and y_0 ($y_0=0.1$ Å) are generated for the initial values of the bond variables $\{y_{i,j}^{(0)}\}$. Then, we start the iteration.

(ii) At the kth step of the iteration, the electronic part of the Hamiltonian is diagonalized by solving Eq. (2.2) for the set of the bond variables $\{y_{i,j}^{(k)}\}$.

(iii) Using the electronic wave functions $\{\phi_{\kappa,s}(i)\}$ obtained above, we calculate the next set $\{y_{i,j}^{(k+1)}\}$ from the left-hand side of Eq. (2.3).

(iv) The iteration is repeated until the sum $\sum_{\langle i,j\rangle}(y_{i,j}^{(k+1)}-y_{i,j}^{(k)})^2$ becomes negligibly small.

III. FULLERENE TUBES WITH FINITE SIZES

In this section, we discuss the variation of the lattice and electronic structures from C_{60} to a tube. We confine the analysis to half-filled systems, where the electron number is equal to the site number N. We calculate for the system size $N=10n$ $(6\le n\le 30)$. The parameters, $t_0=2.5$ eV, $\alpha=6.31$ eV/Å, and $K=49.7$ eV/Å^2, are the same as in previous papers.[2-4] The value of t_0 has been taken from that of graphite. In fact, the phenomenological parameters should be determined for each system with different N. But, their values are not known now. We can certainly assume that the same parameters are valid for all N. Their values should not vary so much even for an infinitely long tube.

Figure 1 shows the bond alternation patterns. Figure 1(a) is the pattern of the infinitely long tube. The front and back views are shown using normal and thin lines, respectively. In our calculations, the conventional Kekulé structure is always the most stable solution when N is sufficiently large. This structure has the alternation of short and long bonds depicted in Fig. 1(a). The length of the unit cell is three times that of the undimerized system. This is a consequence of the fact that the Fermi wave number of the undimerized system is $k_F=2\pi/3a$ (a is the unit cell length of the undimerized system) and the Fermi level is located at the same wave number that the calculation using the local density approximation[9] indicates. The triple length of the new unit cell is thus suggested by the Peierls theorem.

When N is finite, deviations form the above-mentioned Kekulé structure are also observed. We shall consider changes of the alternation patterns shown in Figs. 1(b)–1(e). In these figures, thirty carbons in the left-hand part are arranged like a hemisphere of C_{60}. The other thirty carbons in the right-hand part are arranged similarly. The patterns in these two parts are the same as in C_{60} and C_{70}.[2-4] It is energetically favorable that the parts like the hemisphere of C_{60} always form the same pattern. This is an end effect. The lattice configuration of the finite-N system is determined by the presence of the two ends. When the number of carbon atoms inserted between the two parts is a multiple of thirty, the middle part forms a Kekulé structure. The dimerization is commensurate with the triplicate unit cell. This is realized in Figs. 1(b) and 1(e). For the other numbers of carbon atoms, there are deviations from the Kekulé structure. For example, in Fig. 1(c), there are two rings formed by five short bonds in the middle. In Fig. 1(d), we cannot identify short and long bonds from the length difference in the middle part. These indiscernible bonds are shown by dashed lines. The hexagons formed by the six dashed lines are like a benzene ring which has six bonds of the equal length. There are similar hexagons in C_{70}.[3,4]

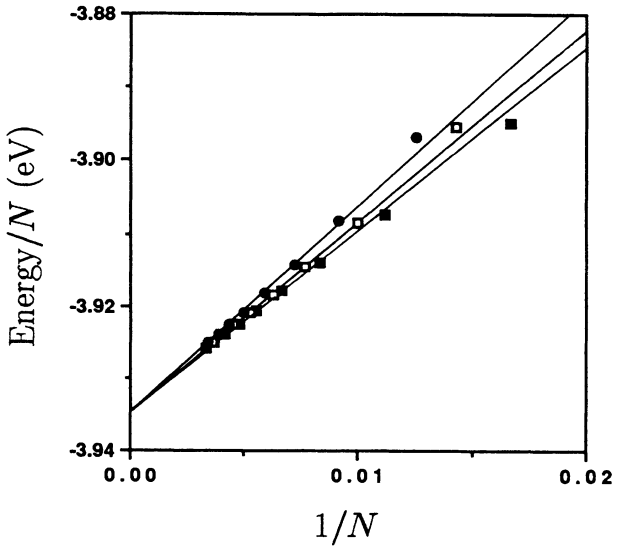

FIG. 2. Total energy per site. The filled squares, open squares, and filled circles are for the series $N=30n$, $30n+10$, and $30n+20$, respectively. Here, n is a integer. The linear lines are extrapolations to infinite N.

The total energy per site is calculated and plotted versus $1/N$ in Fig. 2. There are three series, $N=30n$, $30n+10$, and $30n+20$. Each series is shown by a different symbol. The series $N=30n$ is the most stable of the three. This is due to the Kekulé structure. The other series, which include the defects, have larger energies. Each series is well fitted by a linear line. As N goes to infinity, the energies of the three series come near to the same value: -3.9345 eV. This is the due to the fact that contributions to the total energy from the two ends and the defects become smaller as n increases.

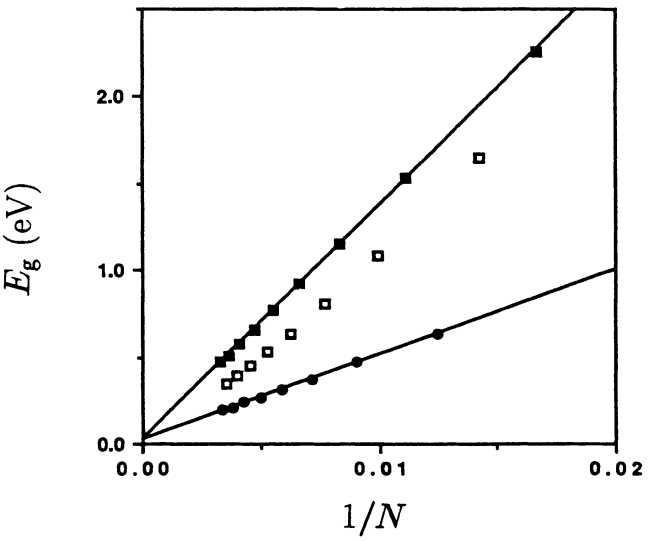

FIG. 3. Energy gap E_g. The filled squares, open squares, and filled circles are for the series $N=30n$, $30n+10$, and $30n+20$, respectively. The linear lines are extrapolations to infinite N.

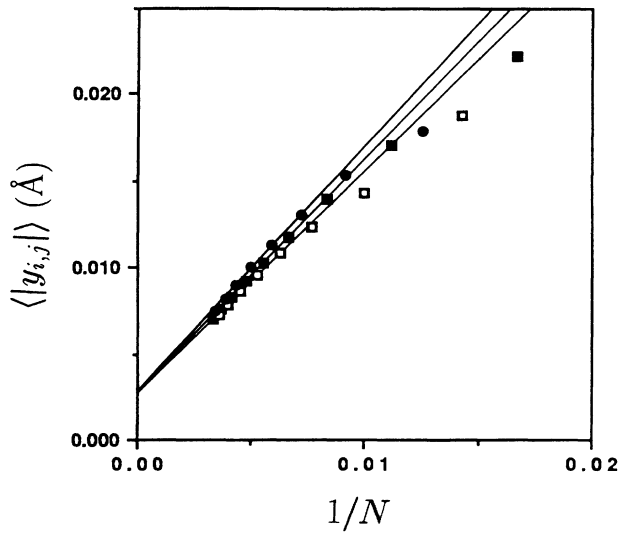

FIG. 4. The average of the absolute value of the bond variable $y_{i,j}$. The filled squares, open squares, and filled circles are for the series $N=30n$, $30n+10$, and $30n+20$, respectively. The linear lines are extrapolations to infinite N.

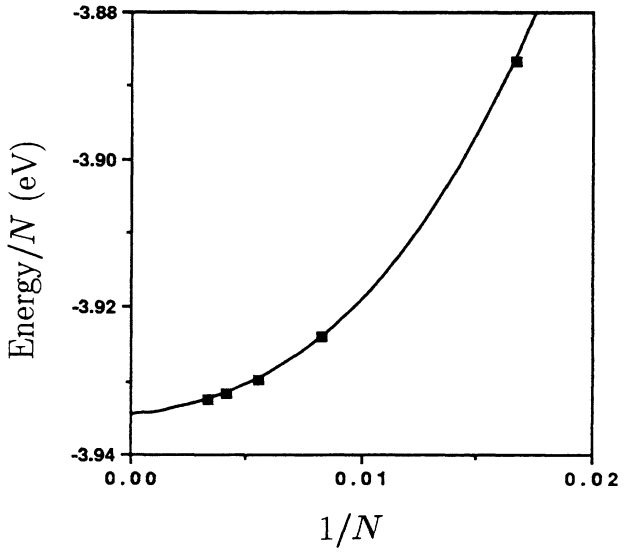

FIG. 5. Total energy per site. The curve is the result of a fitting using a third-order polynomial.

The energy gap E_g, i.e., the energy difference between the HOMO and LUMO, is plotted against $1/N$ in Fig. 3. Again, there are three series. The series $N=30n$ has the largest gap, while the series $N=30n+20$, has the smallest one. The smaller gaps for $N=30n+10$ and $30n+20$ are due to the presence of defects. Extrapolation to $N\rightarrow\infty$ by linear lines is successfully performed to give $\lim_{N\rightarrow\infty}E_g=2.226\times10^{-2}$ eV, which is comparable to kT at room temperature. The infinitely long tube is a semiconductor with a narrow gap.

It is interesting to see what value each bond variable in the Kekulé structure takes as $N\rightarrow\infty$. But, in the present scheme of extrapolation to infinite N, there are always two ends in each system calculated. Dimerization amplitudes in the two end parts are always large. The constraint $\sum_{\langle ij\rangle}y_{i,j}=0$ greatly effects the values of the smaller bond variables at the middle of the tubes. Therefore, extrapolations by the present scheme are not reliable. This problem will be studied in Sec. IV. Instead, we shall calculate the average of the absolute values $\langle|y_{i,j}|\rangle$. This measures the strength of dimerization quantitatively. The result is shown in Fig. 4. Independent extrapolations of the three series to infinite N seem to give the same value: $\lim_{N\rightarrow\infty}\langle|y_{i,j}|\rangle=2.66\times10^{-3}$ Å. The average dimerization for C_{60} is 2.22×10^{-2} Å. The magnitude of the extrapolated value is smaller by one order of magnitude. It would be very hard to observe such small dimerizations. However, the width of the energy gap near room temperature is clear evidence that dimerization remains.

IV. FULLERENE TUBES WITH PERIODIC BOUNDARIES

In this section, we discuss the fullerene tubes calculated with periodic boundary conditions. We consider the system size, $N=60n$ $(1\leq n\leq5)$, where the Kekulé structure shown in Fig. 1(a) is stabilized. This series gives the energy minimum solutions as expected from the discussion in Sec. III.

Figure 5 shows the total energy per site plotted versus $1/N$. The fitting using a third-order polynomial is successful. The result is shown by the curve. The extrapolated value to infinite N is -3.9346 eV.

Figure 6 depicts E_g versus $1/N$. Data points are well fitted by a linear line. The extrapolated value to infinite N is 1.889×10^{-2} eV. This is close to the value 2.226×10^{-2} eV obtained from Fig. 3. We conclude again that an infinitely long tube has a very narrow gap comparable to kT at room temperature.

We shall discuss each bond length at infinite N. Figure 7(a) shows the labels of the bonds. There are four kinds

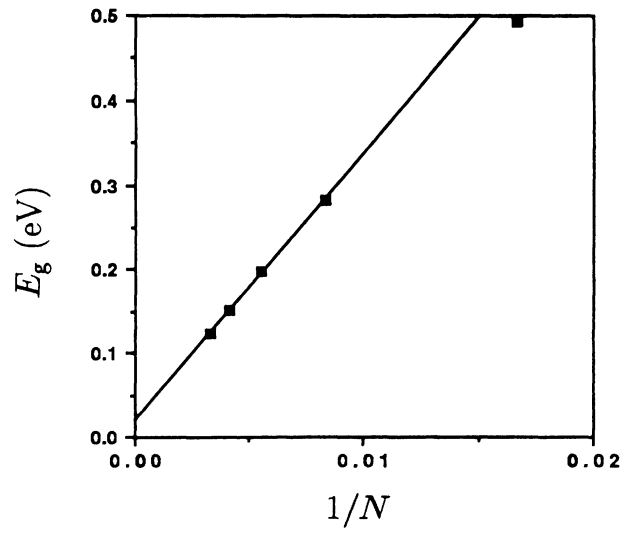

FIG. 6. Energy gap E_g. The linear line is an extrapolation to infinite N.

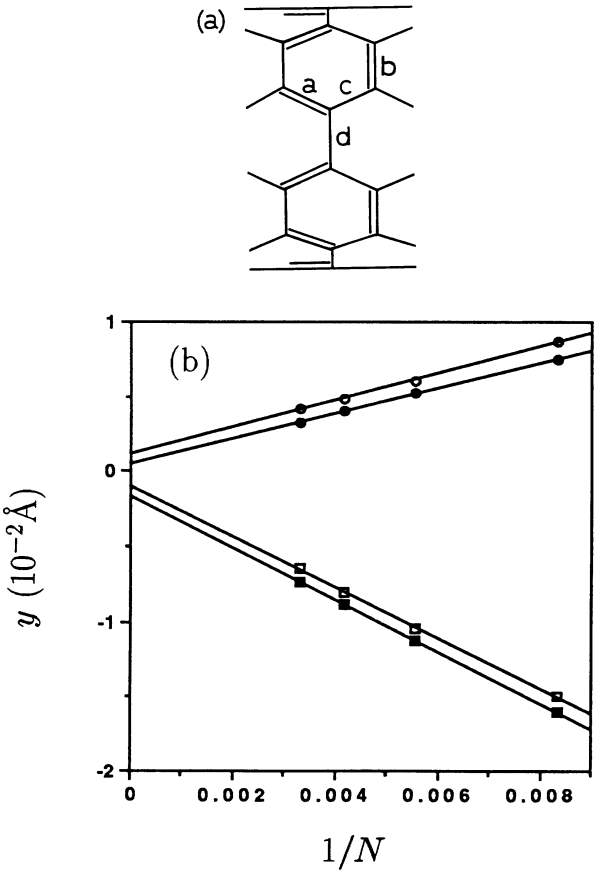

FIG. 7. (a) Labels of nonequivalent bonds. The illustration is a part of the front view of Fig. 1(a). (b) The bond variables. The filled and open squares are for bonds a and b, respectively. The filled and open circles are for bonds c and d. The linear lines are the results of extrapolations.

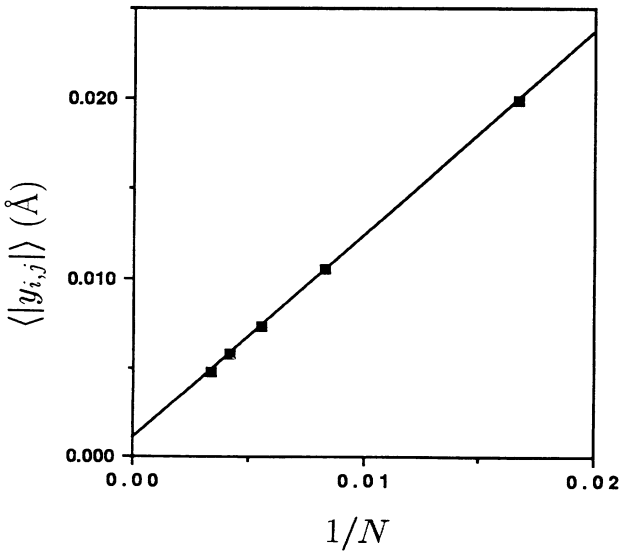

FIG. 8. The average of the absolute value of the bond variable $y_{i,j}$. The linear line is an extrapolation to infinite N.

TABLE I. The bond variables of the infinitely long tube. The labels of bonds are shown in Fig. 7(a). The bond length becomes longer from a to d.

Label of bond	Bond variable (Å)
a	−0.001 645
b	−0.001 002
c	0.000 500
d	0.001 148

of nonequivalent bonds. The length becomes longer from bond a to bond d. Figure 7(b) shows the result of an extrapolation to infinite N making use of linear lines. As far as we judge from the figure, the extrapolation is successful. In Table I, the extrapolated values are listed. All of the values are one order of magnitude smaller than those of C_{60}. It seems that the difference in length between the short and long bonds varies from one author to another and most of the data of C_{60} range between 0.03 and 0.06 Å. The magnitude resolution of the measurements is about 0.01 Å. Thus, it would be very hard to observe the small length differences of Table I in very long tubes. However, we believe that a very small dimerization persists as long as the tube is so long that the conventional Peierls theorem for a one-dimensional system applies.

Finally, we compare the average dimerization with that in Sec. III. We calculate $\langle |y_{i,j}| \rangle$ for each N and plot it against $1/N$ in Fig. 8. The linearly extrapolated value is 9.96×10^{-4} Å. We can also estimate $\langle |y_{i,j_0}| \rangle$ from the data in Table I. The result is 9.54×10^{-4} Å. The two values agree remarkably well. In Sec. III, we have obtained 2.66×10^{-3} Å. The order of the magnitude is the same, but this value is larger than that in this section. This might be due to the effects of the end parts: the dimerization amplitude in the end parts is relatively large and this affects the average value.

V. CONCLUDING REMARKS

We have considered tubes which have nonhelical structures. In this case, the unit cell in the tube axis direction has a simple structure, and interesting dimerization patterns are expected to occur due to the perfect nesting of the Fermi surfaces. In fact, a triplicate length of the unit cell is realized. However, the bond alternations are weaker than those in C_{60} and C_{70}. This is due to the larger carbon number. Similarly, the smaller dimerization than that in polyacetylene is due to the fact that a larger number of carbons are present in the unit cell. Therefore, it would be difficult to observe them directly by experiments. If a very narrow gap comparable to kT near room temperature is observed, this gap would be related to bond alternations.

In the ideal infinitely long tube, the Kekulé structure is triply degenerate. The potential surface among the triple minima might be almost flat. It would be difficult to realize an ordered state. However, in actual samples, the tube is not infinitely long. The length is finite and there

are always two ends. The calculation in Sec. III would simulate the real system better. The phase of the Kekulé structure is uniquely determined by the presence of the end parts. Therefore, the ideal flat energy surface does not smear out the ordered structure in real systems.

We have only calculated dispersion relations for lattice geometries where ten carbons are arranged in a ring perpendicular to the tube axis. In real samples, the number of carbons in a ring can be larger than ten.[1] The dimerizations will become weaker. This should be discussed quantitatively in future works. However, we believe that the nonhelical tubes, which are infinitely long, have dimerization patterns due to the Peierls theorem, even if the strength of bond alternations is very small.

The electronic and lattice structures of helical tubes would be a very interesting problem. When the dimerizations do not occur, the tube will have properties like graphite. Even metallic properties could be expected. When perfect nesting conditions are fulfilled, various dimerization patterns will be realized, depending upon structures of a unit cell (the pitch of the helix and number of carbons in a ring).

---

*Electronic address:
e9118@etlcom1.etl.go.jp,e9118@jpnaist.bitnet.

[1]S. Iijima, Nature **354**, 56 (1991).
[2]K. Harigaya, J. Phys. Soc. Jpn. **60**, 4001 (1991).
[3]K. Harigaya, Chem. Phys. Lett. **189**, 79 (1992).
[4]K. Harigaya (unpublished).
[5]W.-P. Su, J. R. Schrieffer, and A. J. Heeger, Phys. Rev. B **22**, 2099 (1980).
[6]M. Ozaki and A. Takahashi, Chem. Phys. Lett. **127**, 242 (1986); G. W. Hayden and E. J. Mele, Phys. Rev. B **36**, 5010 (1987).
[7]G. E. Scuseria, Chem. Phys. Lett. **180**, 451 (1991); J. Baker, P. W. Fowler, P. Lazzeretti, M. Malagoli, and R. Zanasi, *ibid.* **184**, 182 (1991).
[8]B. Friedman, Phys. Rev. B **45**, 1454 (1992).
[9]J. W. Mintmire, B. I. Dunlap, and C. T. White, Phys. Rev. Lett. **68**, 631 (1992).
[10]R. Saito, M. Fujita, G. Dresselhaus, and M. S. Dresselhaus (unpublished); N. Hamada, S. Sawada, and A. Oshiyama (unpublished).
[11]K. Harigaya and A. Terai, Phys. Rev. B **44**, 7835 (1991).